Clinical Radiology

Texture Analysis of Cardiovascular Magnetic Resonance Cine Images differentiates etiologies of left ventricular hypertrophy

--Manuscript Draft--

Manuscript Number:	CRAD-D-18-00309R1
Full Title:	Texture Analysis of Cardiovascular Magnetic Resonance Cine Images differentiates etiologies of left ventricular hypertrophy
Article Type:	Original Paper
Corresponding Author:	Rebecca Sally Schofield, MBChB Peterborough City Hospital Peterboroough, UNITED KINGDOM
Corresponding Author Secondary Information:	
Corresponding Author's Institution:	Peterborough City Hospital
Corresponding Author's Secondary Institution:	
First Author:	Balaji Ganeshan
First Author Secondary Information:	
Order of Authors:	Balaji Ganeshan
	Rebecca Sally Schofield
	Marianna Fontana
	Arthur Nasis
	Silvia Castelletti
	Stefania Rosmini
	Thomas Treibel
	Charlotte Manisty
	Raymond Endozo
	Ashley Groves
	James Moon
Order of Authors Secondary Information:	
Abstract:	Abstract Background: Textural analysis (TA) shows promise as radiological biomarker. The use of native TA in the field of cardiology is unproven. We hypothesized that Cardiovascular Magnetic Resonance pre-contrast bSSFP cine images could be analysed using TA software; TA features would differentiate different aetiologies of disease causing increased myocardial wall thickness (left ventricular hypertrophy {LVH}) and indicate the severity of myocardial tissue abnormality. Methods: A mid short axis pre-contrast cine frame of 216 cases (50 hypertrophic cardiomyopathy (predominantly LVOTO sub type) (HCM), 52 cardiac amyloid (predominantly AL sub-type) (CA), 68 aortic stenosis (AS), 15 hypertensive with LVH (HTN+LVH) and 31 healthy volunteers (HV)) underwent CMRTA using TexRAD (TexRAD Ltd, Cambridge, UK). Among HV, 16/ 31 were scanned twice to form a test-retest reproducibility cohort. CMRTA comprised a filtration-histogram technique to extract and quantify features using 6 parameters. Results: Test-retest analysis in HV showed a medium filter (3mm) was the most reproducible (intra-class correlation of 0.9 for kurtosis and skewness and 0.8 for mean and SD). Disease cohorts were statistically different ($p<0.001$) to health for all parameters. Pair wise comparisons of CMRTA parameters showed kurtosis and

	skewness consistently significant in ranking degree of difference from HV (greatest to least); CA, HCM, LVH+HTN, AS ($p<0.001$). Similarly mean, SD, entropy and mean positive pixel (MPP) were consistent in ranking degree of difference from HV; HCM, CA, AS and HTN+LVH. Conclusion: Radiomic features of bSSFP CMR data sets, derived using TA, show promise in discriminating between aetiologies of LVH.

Texture Analysis of Cardiovascular Magnetic Resonance Cine Images differentiates etiologies of left ventricular hypertrophy

Rebecca Schofield,[1,2*] Balaji Ganeshan[3*], Marianna Fontana[4], Arthur Nasis[5], Silvia Castelletti[6], Stefania Rosmini[1], Thomas A Treibel[1,2], Charlotte Manisty[1,2], Raymond Endozo[3], Ashley Groves[3*], James C Moon[1,2*]

1. Barts Heart Centre, London, UK
2. Institute of Cardiovascular Science, University College London, UK
3. Institute of Nuclear Medicine, University College London, UK
4. National Amyloid Centre, Royal Free Hospital, London, UK
5. Monash Cardiovascular Research Centre, Monash University Department of Medicine (MMC), Melbourne, Australia
6. Istituto Auxologico Italiano IRCCS, Milan, Italy

* - joint-authors

Short title: Texture analysis in LVH

Author Emails:

rebecca.schofield@doctors.org.uk,b.ganeshan@ucl.ac.uk,m.fontana@ucl.ac.uk,arthurnasis@yahoo.com.au, silvia_castelletti@libero.it, sterosmini@gmail.com, thomas.treibel@gmail.com, cmanisty@gmail.com, raymond_612003@yahoo.com, a.groves@ucl.ac.uk, james.moon@uclh.nhs.uk

Corresponding Author:

Dr Rebecca Schofield
North West Anglia Foundation Trust
Bretton Gate
Peterborough
PE3 9GZ
Email: rebeccaschofield@doctors.org.uk

Competing interests- Dr Balaji Ganeshan is the CEO of TexRad a commercially available software used to analyze the data.

Author Contributions

1. Guarantor of integrity of the entire study; Balaji Ganeshan, Ashley Groves, James C Moon
2. Study concepts and design; Balaji Ganeshan, Ashley Groves, James C Moon, Charlotte Manisty, Arthur Nasis
3. Literature research; Rebecca Schofield
4. Clinical studies; James C Moon, Marianna Fontana, Silvia Castelletti, Stefania Rosmini, Thomas A Treibel
5. Experimental studies / data analysis; Balaji Ganeshan, Raymond Endozo
6. Statistical analysis; Balaji Ganeshan
7. Manuscript preparation; Rebecca Schofield, Balaji Ganeshan, James C Moon
8. Manuscript editing; Silvia Castelletti, Stefania Rosmini, Thomas A Treibel, Charlotte Manisty

Anonymous list of revisions

Dear Editor,

Thank you for your email outlining the reviewers comments.

Pleas find enclosed the revised manuscript. Since this project was first envisaged the field of radio-omics has become an area of increasing research interest. The reviewers constructive criticisms were very helpful and we thank them for their time.

Please see the point-by-point response to the reviewers comments.

Specific points:

1. The introduction section outlines the application of TA to oncological radiomics, but has not mentioned any of the published cardiac applications of TA. There are recent publications of TA application in hypertrophic cardiomyopathy and myocardial infarction that should be referenced in the manuscript.
   References 12,13,14 added.
2. Line 45 - please elaborate what abbreviation SAP scan stands for
   Added to the list of abbreviations
3. Please recheck the number for subsections in Results as they do not appear to run in order
   Order ammended
4. It would help contextualise the data if there is CMR phenotypic or volumetric data for the subjects included in the various disease states - for example, it would be useful to know how significant the LVH is in hypertension cohort or asymmetrical septal hypertrophy is in HCM cohort. Was volumetric and functional data acquired and available for the study subjects?
   Limited data regarding the phenotyping is available. There is a new paragraph to highlight this to the readers
5. Section III of Results where pairwise comparisons of disease states have been made and listed. This section is quite difficult to comprehend apart from the statistically significant p values listed. Please consider alternative presentation of the data, as listing each p value does not really provide any clinical context to the results
   Revision of this section adding in plausible clinical context.
6. Were LGE positive regions included in the analysis of bSSFP segments analysed with TA in the Results section (lines 219-223)?
   Yes
7. The statement in Discussion section where 'this is the first example of the use of TA technique.... (line 280) is incorrect as there are other published applications of non-contrast CMR.
   Ammended
8. In Limitations, it is state that 'the patients in each disease cohort varied in terms of severity of disease'. There has been no corresponding data presented in the manuscript (see Point 4 above)
   Ammended
9. Figure 3 - the patients in the hypertension group have not been included in the Figure. Was this an inadvertent omission?
   Ammended
10. Please consider re-tabulating Table 3 or presenting the data in an easier format to interpret
    The additional explanation in the main body of the text should assist the reader to interpret Table 3

Whilst the concept of applying textural analysis to cardiac pathology in non-contrast CMR is attractive, the data presented does not actually discriminate between the different disease states encompassed. The results are presented in lists of pairwise comparisons that do not provide any clinical context to the disease states or severity of pathology being analysed. Whilst there are statistically significant differences in the parameters presented, these have limited clinical meaning and relevance in current format of

results presented. The statistics performed unfortunately appear to be a 'fishing' exercise for statistically significant p values. There is no CMR phenotypic/volumetric or functional data provided, so it is difficult to know if the statistically significant differences in different disease states analysed by TA actually reflect different clinical phenotypes.

Reviewer 1 comments are welcomed and respected we offer an alternative view point:

Our study is exploratory but not a fishing exercise. We used test-retest cohorts for technical validation which identified SSF 3 to be the most robust and reproducible for CMR. We then performed clinical validation and demonstrated a differ in the parameters between the HV and disease cohorts. We explored the differences in parameters between disease cohorts and gave potential plausible explanation. We took steps to reduce Fahad recovery rate by limiting the statistical comparisons by first deriving the most robust filter size.
In addition, traditional scientific methodology requires the generation of a hypothesis and the derivation of an experiment to test said hypothesis. Use of 'big data' to 'trawl' for pattern recognition turns this ideology on it's head but has led to new scientific developments and the better understanding of diseases. Although we understand the limitations of the study and do not advocate the use of the technique in clinical medicine in it's current form we would advocate further study and better understanding before deciding on clinical utility. We feel it is important that this data is published to ensure scientific progression.

Reviewer #2: Thank you for asking me to review this interesting paper on textural analysis of SSFP cine imaging in CMRI.

I must disclose that I have no experience of textural analysis of medical imaging, however it is becoming increasing clear that we need to maximize the amount of data we draw from our imaging investigations as the processing of large data sets with machine learning becomes more commonplace. The role of CMR in the differentiation of etiologies for myocardial hypertrophy is a particularly rich field for research involving late gadolinium enhancement and parametric mapping. The possibility of interrogating our standard cine images to help in this delineation is very attractive.

I found this paper to be written well with sound methodology, the figures and tables were clear. I would recommend formal statistical analysis due to the volume of data processed.
Formal statistic analysis was performed

As tissue parametric maps are beginning to be accepted as the standard for the evaluation of diffuse hypertrophy I was pleased that the authors proposed evaluating for correlation with these techniques in the methods, unfortunately presumably due to the retrospective nature of this study only ECV in the cardiac amyloid group was available.
This is true

Thank you again for your comments. Please let us know if any further changes are required.

Abstract

Background: Textural analysis (TA) shows promise as radiological biomarker. The use of native TA in the field of cardiology is unproven. We hypothesized that Cardiovascular Magnetic Resonance pre-contrast bSSFP cine images could be analysed using TA software; TA features would differentiate different aetiologies of disease causing increased myocardial wall thickness (left ventricular hypertrophy {LVH}) and indicate the severity of myocardial tissue abnormality.

Methods: A mid short axis pre-contrast cine frame of 216 cases (50 hypertrophic cardiomyopathy (predominantly LVOTO sub type) (HCM), 52 cardiac amyloid (predominantly AL sub-type) (CA), 68 aortic stenosis (AS), 15 hypertensive with LVH (HTN+LVH) and 31 healthy volunteers (HV)) underwent CMRTA using TexRAD (TexRAD Ltd, Cambridge, UK). Among HV, 16/ 31 were scanned twice to form a test-retest reproducibility cohort. CMRTA comprised a filtration-histogram technique to extract and quantify features using 6 parameters.

Results: Test-retest analysis in HV showed a medium filter (3mm) was the most reproducible (intra-class correlation of 0.9 for kurtosis and skewness and 0.8 for mean and SD). Disease cohorts were statistically different ($p<0.001$) to health for all parameters. Pair wise comparisons of CMRTA parameters showed kurtosis and skewness consistently significant in ranking degree of difference from HV (greatest to least); CA, HCM, LVH+HTN, AS ($p<0.001$). Similarly mean, SD, entropy and mean positive pixel (MPP) were consistent in ranking degree of difference from HV; HCM, CA, AS and HTN+LVH.

Conclusion: Radiomic features of bSSFP CMR data sets, derived using TA, show promise in discriminating between aetiologies of LVH.

Introduction

The ability of cardiovascular magnetic resonance (CMR) imaging to aid in tissue characterisation has propelled its use into mainstream clinical cardiology. Late gadolinium enhancement (LGE) imaging and parametric mapping of the myocardium (native T1, T2, T2* and extracellular volume (ECV) maps) offer non-invasive assessment of myocytes and interstitium. These techniques may require the administration of a gadolinium-based contrast agent, additional sequences and breath-holds for the patient. They may be non-specific in early disease. The ability to mine the existing basic data set, using computer algorithms, is an area of current research interest. Each voxel in bSSFP data sets is an expression of the physical structure it represents.

The field of 'Radiomics' is the process of obtaining quantitative data from these qualitative radiological images combined with the use of Artificial Intelligence (AI) this data can be used to create big data sets which can be processed and the data acquired can be linked to patient characteristics and prognostic data. With deep machine learning algorithms this large volume dataset may be used as an ancillary diagnostic tool. Radiomics may even be used to assess response to treatment or to convey certain prognostic characteristics.

Textural analysis (TA) has been used for several decades in many domains. Within medical imaging the technique has generated interest in diverse applications over recent years. In oncology, TA of computed tomography (CT) images has shown correlation to underlying tumor biology by differentiating different histological features (associated with the different hallmarks of cancer) and specific gene mutations.[1-4] In established malignancies, TA relates to tumor histology[5,6] across many common solid tumors (lung, colorectal, oesophageal, breast), it correlates with specific gene mutations and can track therapeutic responses.[7-10] Outside of oncology, non-malignant organ changes can be detected (for example liver cirrhosis and usual interstitial pneumonitis).[11] TA applied to CT, MRI and positron emission tomography (PET)

imaging shows promise in oncological radiomics. Within cardiac imaging CMR-TA has been used to assess the risk of arrhythmia post MI[12] , the use of CMR-TA in pre contrast and LGE imaging of patients with Hypertrophic Cardiomyopathy to predict outcome is a current area of particular interest [13,14].

This project started several years ago at a time when CMRTA had not been reported. We first hypothesised that, routine CMR cine images would be amenable to TA; TA features would differentiate between the different etiologies of disease that cause increased myocardial wall thickness (left ventricular hypertrophy [LVH]) and also healthy controls. Finally we hypothesised CMRTA would provide additional supporting information which may act as a surrogate marker for tissue abnormality by demonstrating correlation between abnormal CMRTA and presence of LGE/increased ECV.

Methods

Study Population

We performed a retrospective analysis of five cohorts of subjects.

All subjects had given informed written consent for their anonymised images being used in clinical research. Analysis was performed on anonymised data from study participants who had previously provided written informed consent for CMR research approved by a local research ethics committee at xxxxxxxxxxxx.

1. Cardiac Amyloid (CA, n=52), confirmed by tissue biopsy, positive SAP scan or cardiac involvement diagnosed by echo criteria.
2. Hypertrophic Cardiomyopathy (HCM, n=50): randomly selected clinically confirmed HCM patients with LVH, predominantly LVOTO subtype (recruited from an ongoing HCM study).
3. Severe Aortic Stenosis (AS, n=68). CMR prior to Aortic Valve Replacement

4. Hypertensive patients with LVH confirmed by increased indexed LV mass on echo (HTN+LVH, n=15).
5. Healthy Volunteers (HV, n=31) all prospectively recruited volunteers with no history of cardiovascular disease (normal health questionnaire, normal electrocardiogram, no cardioactive medication except for primary prevention). This group included 16 healthy volunteers who were scanned twice with deliberate changes to scanning parameters to alter SNR and CNR. This reproducibility testing was performed to identify the most robust CMRTA parameters.

CMR examination

CMR was performed on a 1.5T clinical scanner (Avanto, Siemens Healthcare, Erlangen, Germany) following obtained written consent for anonymised research participation. A mid short axis balanced SSFP pre-contrast cine was acquired in accordance to the Society for CMR (SCMR) guidelines as part of the routine scanning protocol in each study[15]. The ECV was quantified. The contrast agent used was gadoterate meglumine [Dotarem, Guerbet SA, Paris, France] at a dosage of 0.1mg/kg. LGE imaging was performed approximately 10 minutes following administration using either a standard fast low-angle single shot inversion recovery (FLASH) or true fast imaging with steady state free precession sequence (FISP) with a phase sensitive inversion recovery (PSIR) reconstruction. Presence or absence of LGE was reported by an experienced CMR physician (>10 years CMR). For the Amyloid cohort T1 maps and ECV quantification was performed as outlined in previous studies.[16]

In the test-retest cohort of 16 healthy volunteers, a pre-contrast SSFP short axis cine was acquired in accordance to the SCMR guidelines [15]. The volunteer was taken out of the

magnet and repositioned. The piloting and bSSFP SAX cine was then repeated using a different phase encoding direction and FOV. The studies were anonymised and randomised so the CMRTA operator was blinded. This test-retest cohort with altered scanning parameters was employed to assess the variability/reproducibility of CMRTA parameters to simulate the normal routine clinical practice where there will be variation in scanners, scanning protocol between different centres or between serial scans on the same magnet.

CMRTA

CMRTA was assessed using a filtration-histogram technique using a commercially available research software (TexRAD, TexRAD Ltd, www.texrad.com, part of Feedback Plc, Cambridge, UK). [3-10,17] Whole endocardial and epicardial contours were drawn identifying the whole myocardium for analysis. CMRTA comprised an initial filtration-step using a band-pass Laplacian of Gaussian filter (similar to a non-orthogonal Wavelet) to extract and enhance visually imperceptible features corresponding to variation in sizes, number and tonal intensities in relation to the background-tissue/surrounding-pixels defined as fine, medium and coarse texture scales corresponding to the spatial scale filter (SSF). SSF has typically taken the values of 2mm (fine), 3mm (medium) and 6mm (coarse). This was followed by quantification of textures from the filtered intensity maps using histogram based statistical analysis which describes the shape of the histogram. Typical CMR SSFP imaging voxel size is 2.0mmx2.0mmx8.0mm (TR/TE 39.6/1.12ms), flip angle 55 deg, matrix 192x192. Parameters included - mean intensity , standard deviation, entropy, mean of positive pixel (MPP), kurtosis and skewness. Table 1 –Definition of parameters.

Typically, for 'normal' tissue histograms are near Gaussian e.g. kurtosis and skewness near zero. Pathology changes this.[18,19] In brief, 'mean' changes approximately in proportion to the number of objects/features highlighted and their mean brightness (dark objects are negative). MPP only includes pixels greater than zero (i.e bright) and so reduces the impact of dark objects on the mean histogram value. SD increases approximately in proportion to the square root of the number of features highlighted and their mean intensity difference compared with the background (i.e. dark and bright objects are both counted). Skewness is related to the average brightness of the highlighted features, moving away from zero with intensity variation in highlighted features and towards zero with an increasing number of features highlighted. Kurtosis is inversely related to the number of features highlighted (whether bright or dark) and increases by intensity variations in highlighted features. Entropy reflects how irregular or 'random' the pixel intensity distribution is. Figures 1 illustrates the workflow of undertaking the CMRTA.

Statistical Analysis

IBM SPSS Statistics (version 22, Chicago, Illinois) was used for statistical analysis. Test-retest (reproducibility) of the CMRTA parameters across the 3 SSF values (fine, medium, coarse) was evaluated using the intra-class correlation (ICC). ICC>0.75 were considered to be reproducible. Bland-Altman plots were used to visualise the average-difference plot for the CMR parameters. Amongst the three different SSF values representing fine, medium and coarse texture scales, one which demonstrated the texture parameters to be most robust (based on the above reproducibility analyses) were further evaluated for their clinical diagnostic capabilities. For each disease sub-types, and each preselected texture parameter, box and whisker plots were generated with non-parametric pairwise Kruskal Wallis and Mann Whitney

testing to identify pairwise differences. ROC analysis was performed to assess the sensitivity and specificity of each parameter in differentiating AS from HTN+LVH on the basis of CMRTA alone.

Mann Whitney test was used to assess any of the derived texture parameters could differentiate between LGE positive versus negative. Spearman's rank correlation test was used to identify if there was a correlation between ECV and any of the derived textural parameters. P-value of <0.001 was regarded as significant.

With 5 conditions, 3 filters and 6 parameters, multiple pairwise parameters are possible so to avoid issue related to multiple testing and false discovery rate, we selected to pursue the most reproducible parameters (using the test-retest reproducibility assessment in the healthy volunteers as a marker of information extraction rather than scatter).

Results

Given the number of components to this preliminary study the results are presented in the order of Test-restest analysis (to inform the most reproducible filter size), Comparison of the parameters derived in HV vs all disease groups, the results of comparison between the disease states and finally the analysis with the disease cohorts of HCM and CA of patients with different clinical phenotypes.

I. Test re-test analysis

Comparing filters, the medium (spatial scale factor, SSF=3mm) filter was the most reproducible (example: ICC for Mean, SD, skewness and kurtosis were 0.84, 0.75, 0.92 and 0.87 respectively, average ICC= 0.85). Average ICC of the same parameters for fine (2mm) was 0.70 and coarse (6mm) was 0.76.

Bland-Altman plots for Mean, SD, skewness and kurtosis using SSF 3 for the test-retest cohort

is shown in Figure 2.

Absolute values for the 6 derived parameters in HV and each disease state are shown in Table 2 (all figures to 2 decimal places) and Figure 3.

Accordingly only texture quantifiers at medium filter (SSF 3mm) was pursued further for statistical analysis to evaluate clinical diagnostic capabilities.

II Health vs Disease (Figure 3)

Figure 3 highlights that the parameters can be positive or negative so we assessed degree of change from zero. Within our study mean and skewness were generally negative, suggesting more dark objects were highlighted in all cohorts, whereas SD, entropy and MPP were generally positive. By definition SD and MPP should be positive. The fact that entropy was positive suggests a degree of irregularity within the myocardium. Kurtosis, indicates the visual contrast. A high/positive kurtosis indicates a greater range of contrast and a low/negative kurtosis indicates a narrower range of visual contrast.

Comparing the 4 disease states (CA, HCM, AS, HTN+LVH), to health (HV), the mean, SD, MPP and entropy showed the greatest difference from zero in the HV whereas kurtosis and skewness were closest to zero in HV. This may suggest that in HV there is a narrower range of visual contrast and that there is a normal distribution curve of the pixel intensities in HV.

Between disease conditions the greatest differences in parameters from health were in HCM (mean, SD, entropy, MPP) and CA (kurtosis, skewness). Specifically - HCM and CA were most different to health (all six texture parameters statistically different, each $p<0.001$); then AS (5 parameters were different $p<0.001$; entropy was not), and HTN+LVH (5 were different - mean, SD, entropy, and kurtosis, each $p<0.001$, MPP $p<0.002$).

The histological processes in CA and HCM differ, however, it is likely that the degree of myocardial abnormality in the CA and HCM cohort would be greater then in the AS and HTN+LVH cohorts.

Broadly speaking in CA there is an expansion of the myocardial interstitial matrix as a result of abnormal protein deposition. There is a predilection for subendocardial involvement, however, when compared to HCM there is more likely to be a relatively uniform degree of abnormality compared to healthy myocardium. The finding that CA showed the largest range of pixel visual contrast (kurtosis) and skewness may suggest the detection of a 'granularity' and degree of average brightness of the pixels.

Broadly speaking in HCM there is diffuse myocardial fibrosis and myofibril disarray with patches of focal interstitial fibrosis. This would make HCM the most 'random' pathology in terms of the disease pattern within the myocardium. The finding that entropy was the most different to HV therefore has potential plausible explanation.

III Comparing Disease States-Pairwise comparisons (Figure 4/Table 3)

Table 3 highlights the pair-wise comparison of the study cohorts. Figure 4 demonstrates box and whisker plots for the CMRTA derived parameters across the cohorts.

Within the 4 diseases differences (6 pairs), the following results were observed:

a. HCM vs CA

Mean ($p=0.019$) and skewness ($p=0.002$) were negative and nearer to zero (i.e. 'higher') in HCM compared to CA. SD ($p<0.001$), entropy ($p<0.001$), MPP ($p=0.002$) and kurtosis ($p=0.026$) were positive and nearer to zero (i.e. 'lower') in HCM compared to CA.

The pixel brightness was therefore higher in HCM. The pixel brightness, the number of abnormal features highlighted and the degree of irregularity were all higher in HCM. The range of pixel visual contrast was higher in CA.

b. HCM vs AS

Mean ($p<0.001$) and skewness ($p=0.095$, NS) were negative with Mean being nearer to zero (i.e. 'higher') whereas Skewness showed a greater deviation from zero (i.e.'lower') in HCM compared to AS.

SD ($p<0.001$), entropy ($p<0.001$) and MPP ($p<0.001$) were positive and nearer to zero (i.e. 'lower') in HCM compared to AS. Kurtosis ($p<0.001$) was positive and away from zero (i.e. 'higher') in HCM compared to AS.

Therefore, compared to AS, HCM showed fewer objects highlighted but a larger range of pixel intensities and a higher degree of irregularity.

c. CA vs AS

Mean ($p<0.001$) and skewness ($p<0.001$) were negative with Mean being closer to zero (i.e. 'higher'). Skewness, showed a greater deviation from zero (i.e. 'lower') ($p<0.001$) in CA compared to AS.

SD ($p<0.001$), entropy ($p=0.001$), MPP ($p<0.001$) were all positive and were nearer to zero (i.e. 'lower') in CA compared to AS. Kurtosis ($p<0.001$) was also positive and more deviated from zero in CA (i.e. 'higher') compared to AS.

Therefore compared to AS, CA showed fewer number of features highlighted but a larger range of pixel intensities and a higher degree of irregularity.

d. HCM vs HTN+LVH

Mean ($p=0.064$) was negative and closer to zero (i.e. 'higher') in HCM compared to HTN+LVH ($p=0.064$). Skewness was also negative with a greater deviation from zero in HCM (i.e. 'lower'), ($p=0.001$) compared to HTN+LVH.

SD (p=0.035), entropy (p=0.012) and MPP (p<0.001) were all positive and all were lower in HCM compared to HTN+LVH.

Kurtosis showed a trend to be higher in HCM compared to HTN+LVH but did not reach statistical significance, (p=0.162).

Interestingly the difference between the range of pixel intensity highlighted was not statistically different between the HCM and HTN+LVH cohorts. The pixel brightness and degree irregularity was greater in the HCM group.

e. CA vs HTN+LVH

Mean was negative and showed a trend to be further from zero (ie 'lower') in CA compared to HTN+LVH but did not reach significance (p=0.874).

MPP (p=0.003) and skewness (p<0.001) were positive and significantly closer to zero (i.e. lower) in CA compared to HTN+LVH. Kurtosis was positive and higher in CA, (p=0.002).

SD (p=0.198) and entropy (p=0.134) were negative and closer to zero (i.e. lower) in CA compared to HTN+LVH but did not reach statistical significance.

The degree of pixel brightness was higher in the CA cohort but the number of features highlighted was lower. Perhaps this may explain why the entropy did not reach statistical significance.

f. AS vs HTN+LVH

Mean (p<0.001) and skewness (p=0.002) were negative and further from zero (i.e. 'lower') in AS than HTN+LVH.

SD (p<0.001) and entropy (p<0.001) were positive and further from zero (i.e. 'higher') in AS compared to HTN+LVH. MPP (p=0.767) showed a trend to be lower in AS compared to HTN+LVN but did not reach statistical significance.

Kurtosis (p=0.041) was lower in AS compared to HTN+LVH.

The degree of irregularity and the range of pixel intensities was higher in the AS group, perhaps suggesting more severe disruption to the myocardium (myocytes and extra-cellular matrix).

The strongest results could generate ROC curves eg HCM (most change in parameters from HV) vs AS (least change in parameters from HV).

A mean >= -97.64 identified HCM from AS with a sensitivity of 72% and specificity of 94% (AUC=0.89, p<0.001, Figure 5). A kurtosis >= 1.3550 identified HCM from AS with a sensitivity of 72.0% and specificity of 69.1% (AUC=0.75, p<0.001). A SD < 158.5550 identified HCM from AS with a sensitivity of 75.0% and specificity of 78.0% (AUC=0.86, p<0.001). An entropy < 5.9000 identified HCM from AS with a sensitivity of 72.1% and specificity of 78.0% (AUC=0.87, p<0.001). A MPP < 46.7600 identified HCM from AS with a sensitivity of 71.0% and specificity of 78.0% (AUC=0.81, p<0.001).

IV. Disease subgroups: LGE in HCM and ECV in CA

Clinical phenotypic data was not routinely collected for the purposes of this preliminary study. For the disease cohorts of HCM and CA clinical phenotypic data in the form of HCM LGE+/- and CA ECV was available. Comparison of the parameters showed that in HCM, mean was significantly higher (p=0.031) and MPP was significantly lower (p=0.045) in LGE +ve compared to LGE -ve group. Figure 5.

For CA, the correlation between kurtosis and ECV was not significant (rs=0.222, p=0.193, n=36) however the numbers were small.

Discussion

Within the cardiac phenotyping techniques available, imaging plays a major role, and CMR adds value because it can characterize the myocardium using techniques like advanced LGE and parametric mapping and ECV quantification. In this preliminary study, we show;

1. CMR images are amenable to TA.

2. CMRTA can differentiate between HV and disease. Specifically - HCM and CA were most different to health (all six texture parameters statistically different, each $p<0.001$); then AS (5 parameters were different $p<0.001$; entropy was not), and HTN+LVH (5 were different - mean, SD, entropy, and kurtosis, each $p<0.001$, MPP $p<0.002$).

3. CMRTA parameters showed significant differences between diseases. Specifically- mean and entropy were found in the HCM vs CA; SD, entropy, MPP and kurtosis in HCM vs AS; skewness and MPP in HCM vs HTN+LVH; all parameters in CA vs AS; skewness in CA vs HTN+LVH and mean, SD and entropy in AS vs LVH+HTN.

It is plausible to believe that the myocardial structure varied the most to 'normal myocardium' in the HCM and CA. The pattern of myocardial involvement is different between HCM and CA and entropy reflects the degree of irregularity within the myocardium.

Further information regarding myocardial texture captured by images from standard cines may not be appreciated by the human eye but may be detected using TA software and eventually large volume data set machine learning could enable automated tissue characterization.

Myocardial TA, in this study was most robust and richest using a medium filter (3mm domain) – just above pixel size.

Myocardial TA may have promise in detecting differences between aetiology of myocardial diseases and also for risk stratifying within a disease and assessing response to therapies. One study has shown correlation of CMRTA features to arrhythmia risk post MI.[16]

Multiple derived parameters in newer machine based visual assessment techniques are challenging to rationalize. The statistical output from the filtration-histogram MRTA technique such as mean, standard deviation, kurtosis, skewness, mean positive pixels and entropy, may not be intuitive to comprehend but they are conventional descriptors for histogram distribution. With so many possible correlations, we followed a "nested" approach, starting with test-retest data to identify the most reproducible filter scale (medium-texture at SSF=3mm) followed by texture quantification at that scale to differentiate between the healthy and 4 diseased states as well as between the diseased states and with 2 "histological" correlations (ECV and LGE). We found biologically plausible associations – with Amyloid and HCM being much more abnormal than other disease – a hierarchy that has credibility against known pathological differences.

The MRTA derived parameters may provide supporting evidence of the degree of myocardial abnormality and the uniformity of that process throughout the myocardium.

Whist the techniques are not refined enough currently to give a diagnosis, this area is worth exploring further. The benefits of TA is that large data sets, which are routinely acquired, can be processed and the data acquired can be linked to patient characteristics and prognostic data. With deep machine learning algorithms this large volume dataset may be used as an ancillary diagnostic tool or prognostic indicator. Certainly it presents an opportunity for potential development. The benefits of this technique are that it is fast and easy to perform and does not require additional scanning time, sequences or administration of gadolinium based contrast agents. It could complement more conventional imaging approaches and provide a more sensitive marker of degree of myocardial microstructure disruption/abnormality. With the increasing use of 'big data' sets and machine learning it may be possible to decode these

numerous statistical outputs from TA to provide a more clinically relevant and useable outcome.

We found in our study the medium texture scale to be robust from reproducibility point of view and the texture quantifiers at medium texture scale such as kurtosis, MPP, mean and skewness in particular to demonstrate diagnostic capability.

TA has been successful in the fields of oncology [2-9,17], enabling earlier diagnosis of malignancy and as an imaging biomarker, linking imaging to genetic basis of malignancy and tracking response to treatment. In addition various studies have shown benefit of TA in the detection of liver fibrosis with both MR and CT.

This is a preliminary study and further research is required to fully define the role of this technique which is rapid to perform. The strength is in the use of images which are routinely obtained without use of IV gadolinium based contrast. It has major potential in large volume studies involving retrospective analysis of scans and outcome data.

Study Limitations

This project, being a single centre study with small numbers, is a pilot study. The majority of scans were performed over several years using the same magnet. The patients in each disease cohort are likely to vary in terms of severity of disease however, clinical phenotypic data was not recorded for the study populations. Data regarding myocardial function and patient outcome is also missing.

Due to the numerous statistical comparisons the possibility of chance findings of statistical significance are high.

The ROI used was the whole mid ventricular slice on SSFP imaging in diastole, within a disease process the histological features are unlikely to be uniform throughout the myocardium.

CMRTA is therefore more suited to conditions which affect the myocardium in a diffuse and largely uniform manner. There are also limitations due to movement and blood flow. The spatial resolution of CMRTA is 1mm.

Despite this the test retest reproducibility cohort data was encouraging and across all parameters there was difference between the pathologies and healthy volunteers.

Conclusion

CMRTA is a candidate clinical and research tool to describe myocardial structural disarray. It may be of patient benefit across a variety of conditions which affect the myocardium in terms of early diagnosis, prognosis and follow up of serial change following interventions and therapies. Further evaluation on large volume data sets from CoreLabs should be pursued.

List of abbreviations

LGE	Late gadolinium enhancement
CMR	Cardiovascular Magnetic Resonance
CMRTA	Cardiovascular Magnetic Resonance Textural Analysis
SSFP	Steady state free precession
CA	Cardiac Amyloid
AS	Aortic Stenosis
LVH	Left ventricular hypertrophy
HTN	Hypertension
HV	Healthy volunteers
AL-subtype	Amyloid light chain
LVOTO	Left ventricular outflow tract obstruction
MPP	Mean positive pixel
SD	Standard deviation
ECV	Extra-cellular volume
TA	Textural Analysis
SNR	Signal to noise ratio
CNR	Contrast to noise ratio
PSIR	Phase sensitive inversion recovery
FLASH	Fast low-angle single shot inversion recovery
FOV	Field of view
SCMR	Society of Cardiovascular Magnetic resonance
ICC	Intra-class correlation
PET	Positron Emission Tomography
SAX	Short axis stack
SAP	Serum Amyloid P component

Declarations

Ethical Approval and Consent to participate- not applicable.
Analysis was performed on anonymised data from study participants who had previously provided written informed consent for CMR research approved by a local research ethics committee at xxxxxxxxxxx

Consent for publication- not applicable

Availability of supporting data- not applicable

References

1. Kassner A, Thornhill RE. Texture Analysis: A review of neurological MR imaging applications. Am J Neuroraiol. 2010:31:809-816.
2. Skogen K, Ganeshan B, Good C et al. Measurements of heterogeneity in gliomas on computed tomography relationship to tumour grade. J Neurooncol. 2013:111:213-219.
3. Ganeshan B, Abalake S, Young RC et al. Texture Analysis of non-small cell lung cancer on unenhanced computed tomography: initial evidence for a relationship with tumour glucose metabolism and stage. Cancer Imaging 2010:10:137-143.
4. Sieran JC, Smith AR, Thiesse J et al. Exploration of the volumetric composition of human lung cancer nodules in correlated histopathology and computed tomography. Lung Cancer. 2011:74:61-68.
5. Ganeshan B, Goh V, Mandeville HC et al. Non-small cell lung cancer. Histopathological correlates for textural parameters on CT. Radiology 2013:266:326-336.
6. Ganeshan B, Panayiotou E, Burnard K et al. Tumour heterogeneity in non-small cell lung carcinoma assessed by CT texture analysis: a potential marker of survival. Eur Radiol 2012;22:796-802.
7. Win T, Miles KA, James SM et al. Tumour heterogeneity and permeability as measured on the CT component of PET/CT predicts survival in patients with non-small cell lung cancer. Clin Cancer Res 2013;19:3591-3599.
8. Ahmed A, Gibbs P, Pickles M et al. Texture analysis on assessment and prediction of chemotherapy response in breast cancer. J Magn Reson Imaging. 2013:38:89-101.
9. NG F, Ganeshan B, Nathan P et al. Assessment of primary colorectal cancer heterogeneity by using whole-tumour texture analysis: contrast enhanced CT texture as a biomarker of 5 year survival. Radiology 2013;266:177-184.

10. Lopes R, Ayache A, Makni N et al. Prostate cancer characterisation on MR images using fractal analysis. Med Phys 2011:38:83-95.
11. Depeuringe A, Chin AS, Leug AN eta al. Automated classification of UIP using a regional volumetric analysis in high resolution computed tomography. Investigate Radiology. 2015. 50,4: 261-267.
12. Kotu LP, Engan K, Borhani R, Katsaggelos AK, Ørn S, Woie L, Eftestøl T. Cardiac magnetic resonance image-based classification of the risk of arrhythmias in post-myocardial infarction patients. Artif Intell Med. 2015 Jul;64(3):205-15.
13. Cheng S, Fang M, Cui C, Chen X, Yin G, Prasad SK, Dong D, Tian J, Zhao S. LGE-CMR-derived texture features reflect poor prognosis in hypertrophic cardiomyopathy patients with systolic dysfunction: preliminary results. Eur Radiol. 2018 May 4.
14. Baeßler B, Mannil M, Maintz D, Alkadhi H, Manka R. Texture analysis and machine learning of non-contrast T1-weighted MR images in patients with hypertrophic cardiomyopathy-Preliminary results. Eur J Radiol. 2018 May;102:61-67.
15. Kramer CM, Barkhausen J, Flamm SD, Kim RJ, Nagel E: Standardized cardiovascular magnetic resonance imaging (CMR) protocols, society for cardiovascular magnetic resonance: board of trustees task force on standardized protocols. J Cardiovasc Magn Reson. 2008, 10: 35-10.1186/1532-429X-10-35.
16. Blinded for review
17. Ozkan E, West A, Dedelow JA et al. CT gray-level texture analysis as a quantitative imaging biomarker of Epidermal Growth Factor Recptor mutation status in adenocarcinoma of the lung. Am J Roentgenol. 2015;205:1016-25.
18. Miles KA, Ganeshan B, Hayball MP. CT textural analysis using the filtration-histogram method: what do the measurements mean? Cancer Imaging. 2013;13:400-6.
19. Sala E, Mema E, Himoto Y et al. Unravelling tumour heterogeneity using next-generation imaging: radiomics, radiogenomics and habit imaging. Clinical Radiology 2017;72:3-10.

Table List

Table 1: A table outlining all the CMRTA derived texture parameters and their meaning.

Table 2: Table showing the average values to 2 decimal places of the 6 parameters for each of the disease states and HV, using Spatial Filter Size 3.

Table3: Table showing the pair-wise comparison of all study cohorts and the parameters showing statistical significance

Figures List

Figure 1: Illustrates the TexRad histogram-filtration method of CMR image analysis workflow.

Figure 2: Bland-Altman plots for Mean, SD, skewness and kurtosis using SSF 3 for the test-retest cohort**.**

Figure 3: Bar graph showing the average values of the 6 parameters for each of the disease states and HV, using Spatial Filter Size 3.

Figure 4: Using the medium scale, Figure 4 demonstrates box and whisker plots for CMR texture parameters of mean, standard deviation, entropy and kurtosis across all disease types (HCM, CA, AS, HV, HTN+LVH). 0=HCM, 1=CA, 2=AS, 3=HV, 4=HTN+LVH

Figure 5: ROC-analysis HCM vs AS using Mean. A mean >= -97.64 identified HCM from AS with a sensitivity of 72.0% and specificity of 94.1% (AUC=0.89, $p<0.001$) .

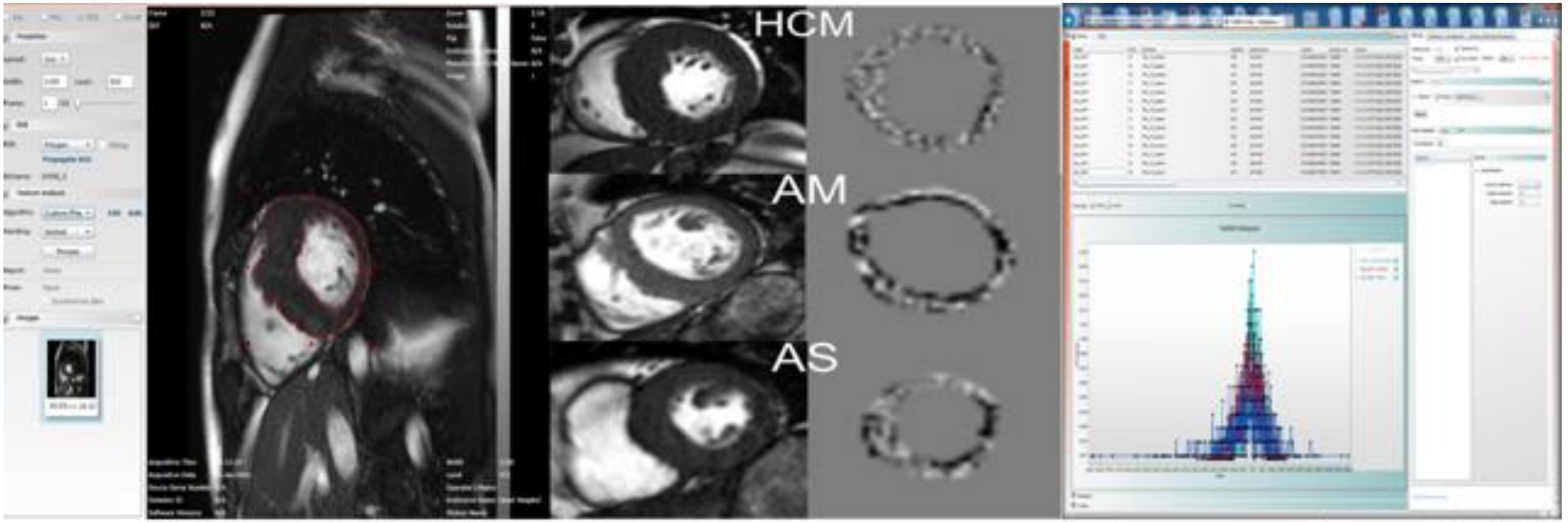

Study series is imported into the TexRad package. The mid ventricular slice of the SAX stack SSFP is chosen for analysis. A ROI (red outline) of the entire myocardium is drawn.

From the SSFP image the TexRad software extracts the data voxel by voxel. A Laplacian of Gaussian filter (similar to a non-orthogonal Wavelet) is applied to extract and enhance visually imperceptible. Each voxel is unique in terms of its intrinsic properties.

Features corresponding to variation in sizes, number and tonal intensities in relation to the background-tissue/surrounding-pixels data contained by each voxel is displayed. This data is then analysed in statistical terms and expressed using the 6 parameters outputs of:
Mean, SD, entropy, kurtosis, MPP and skewness

Figure 2: Bland-Altman plots for Mean, SD, skewness and kurtosis using SSF 3 for the test-retest cohort.
Blinded analysis of each scan performed by single operator. Same patient was scanned twice deliberately changing scan parameters (Phase encoding direction, FOV, re-piloted).

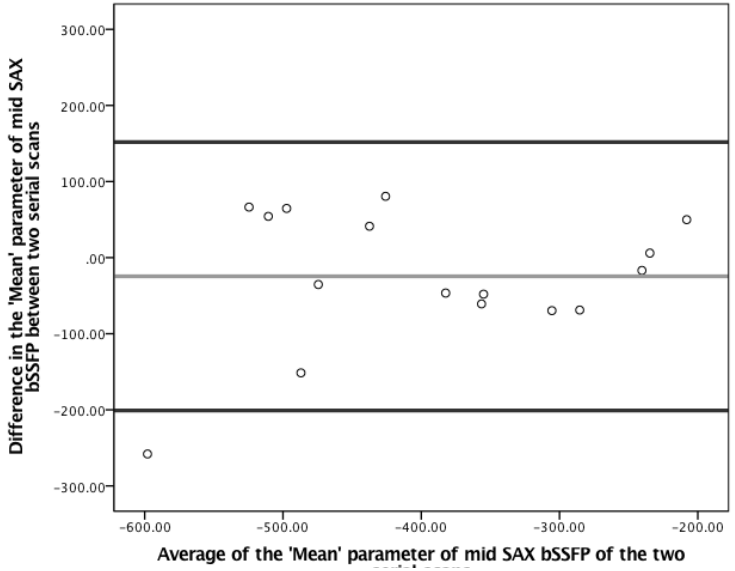

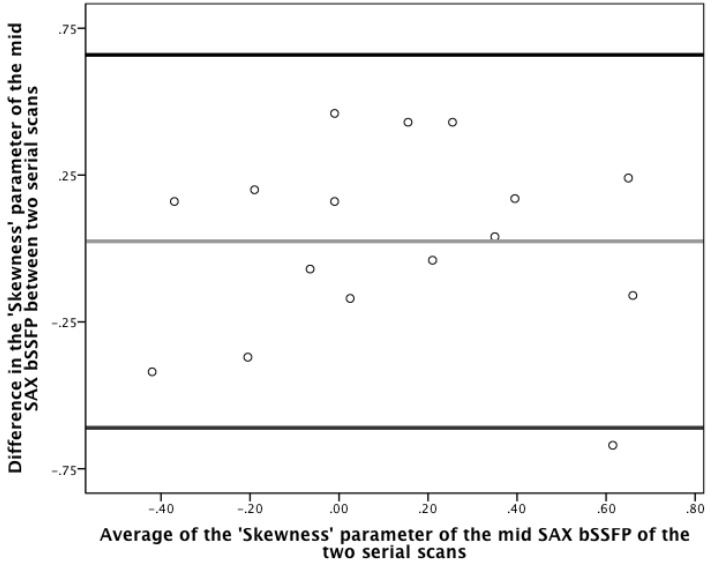

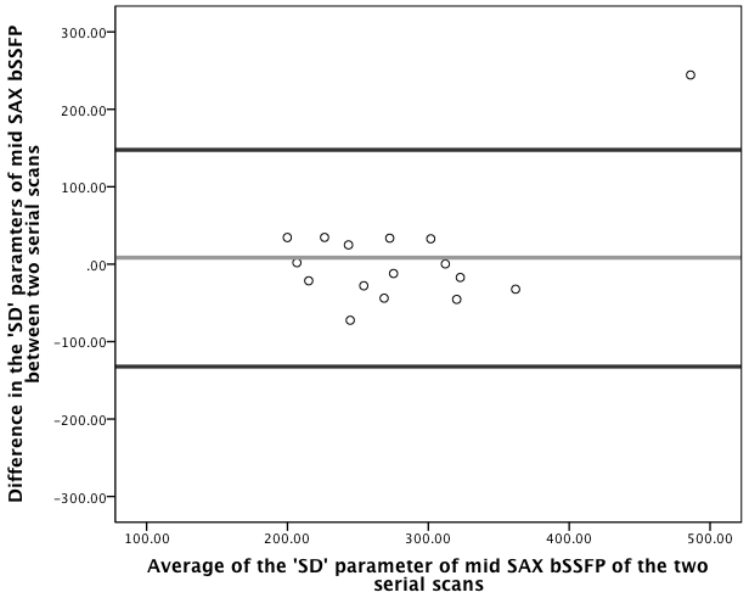

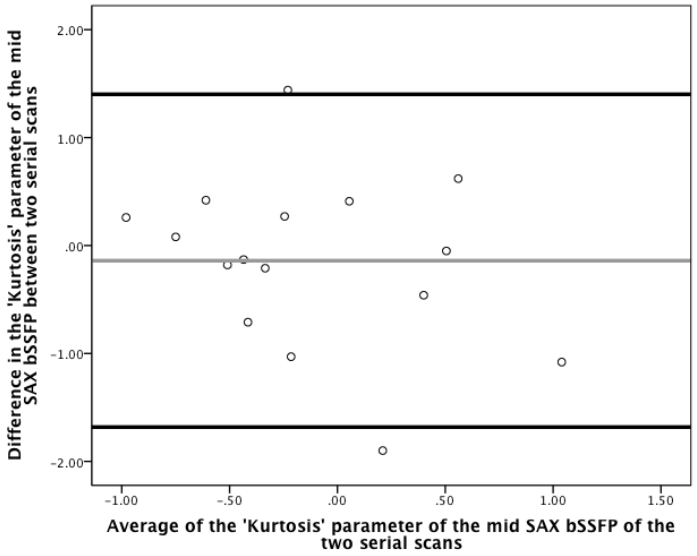

Figure 4: Using the medium scale, Figure 4 demonstrates box and whisker plots for CMR texture parameters of mean, standard deviation, entropy and kurtosis across all disease types (HCM, CA, AS, HV, HTN+LVH). 0=HCM, 1=CA, 2=AS, 3=HV, 4=HTN+LVH

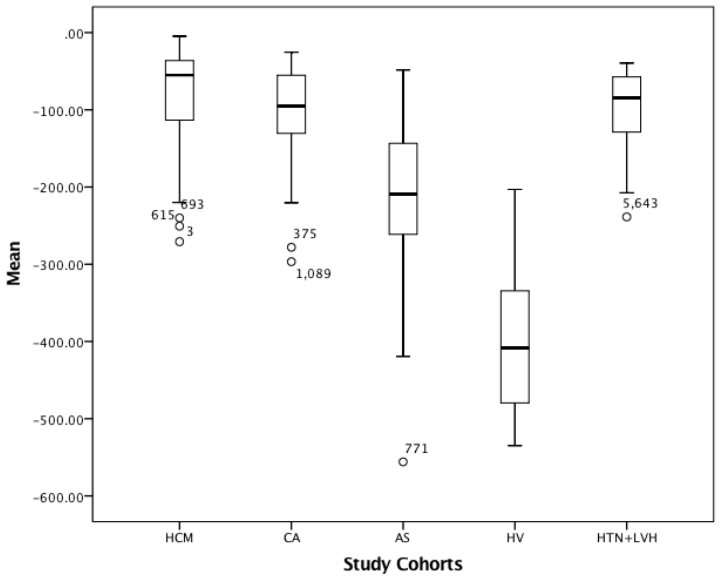

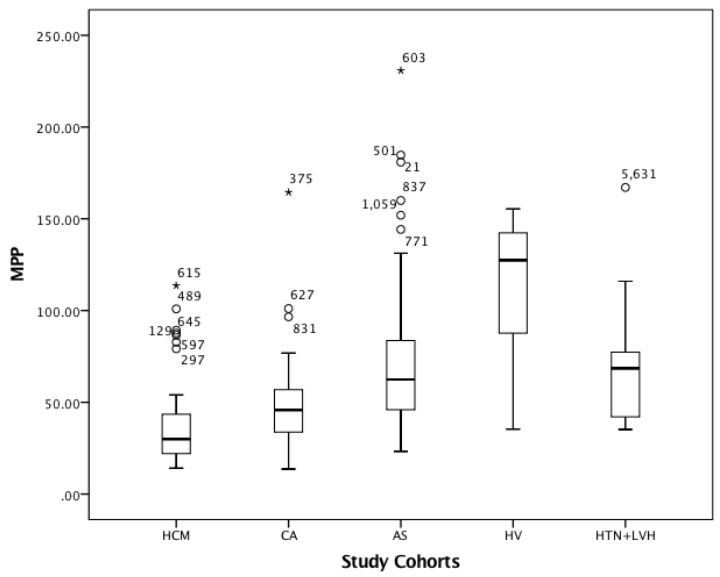

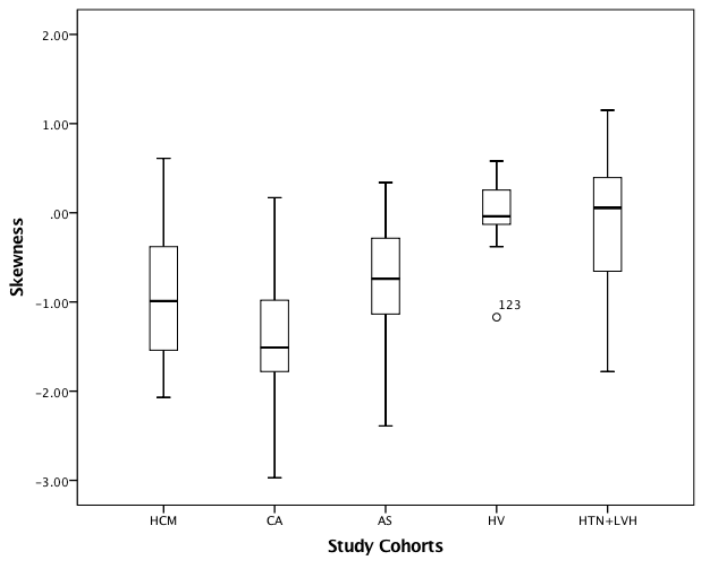

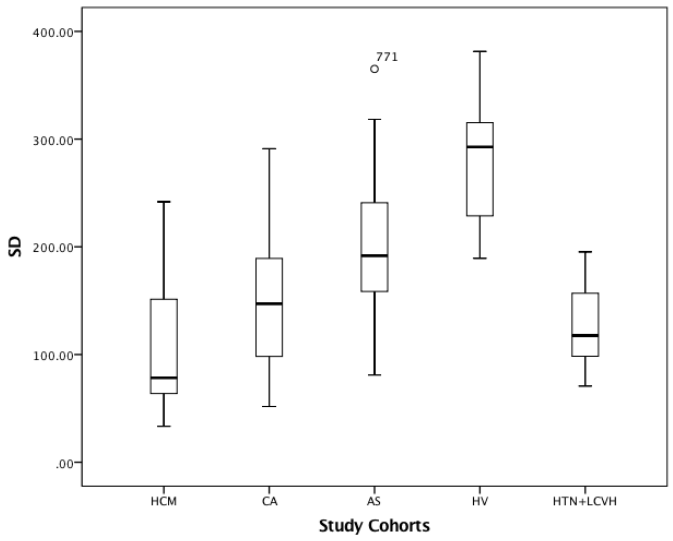

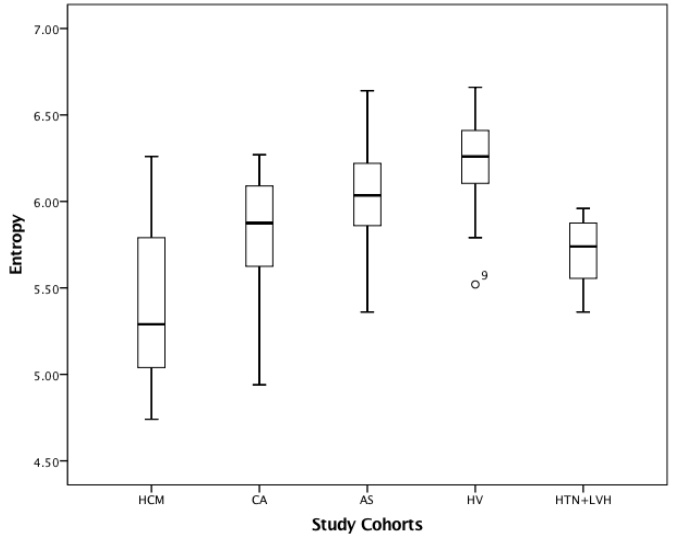

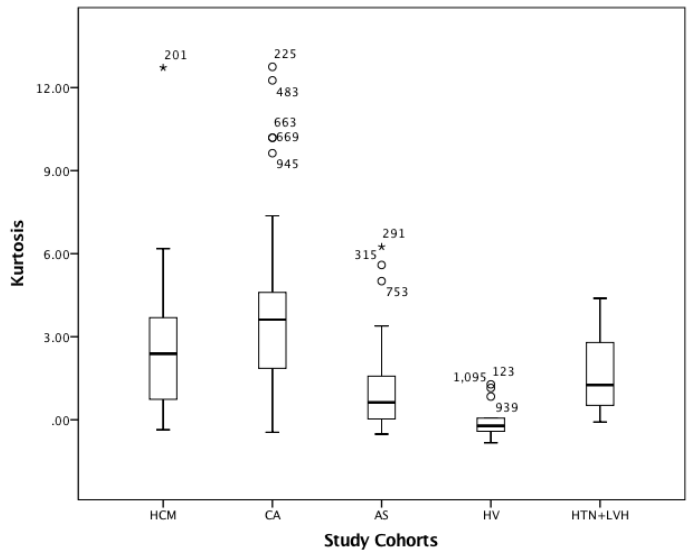

Figure 5 *ROC-analysis HCM vs AS using* Mean

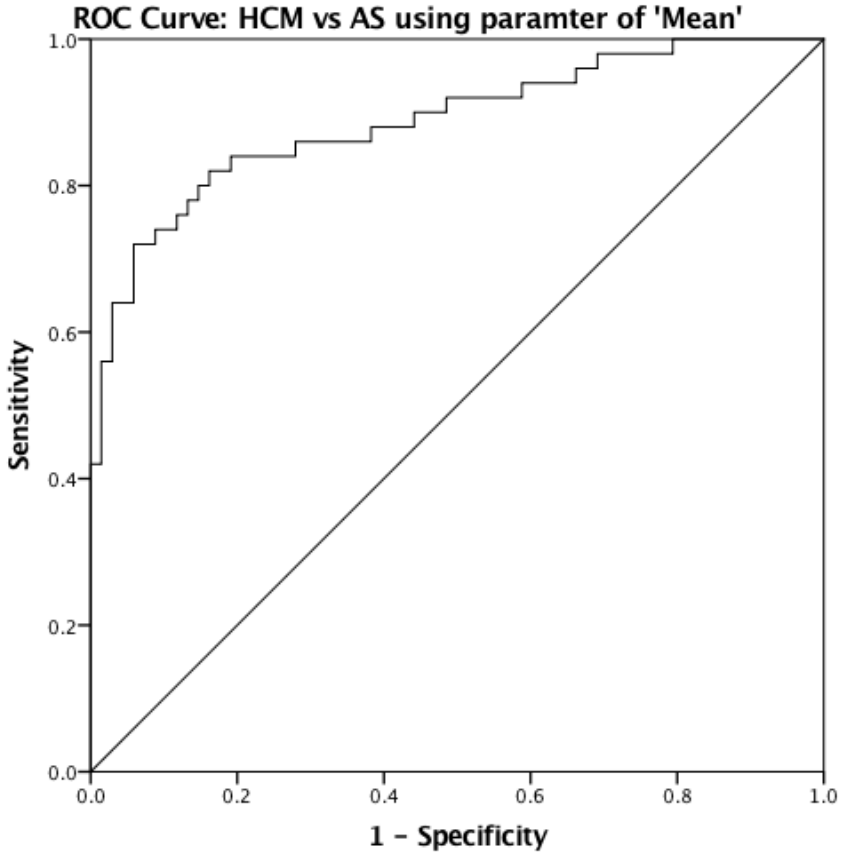

A mean >= -97.64 identified HCM from AS with a sensitivity of 72.0% and specificity of 94.1% (AUC=0.89, p<0.001.

Revised Figure

Figure 3: Bar graph showing the absolute values of the 6 parameters for each of the disease states and HV, using Spatial Filter Size 3.

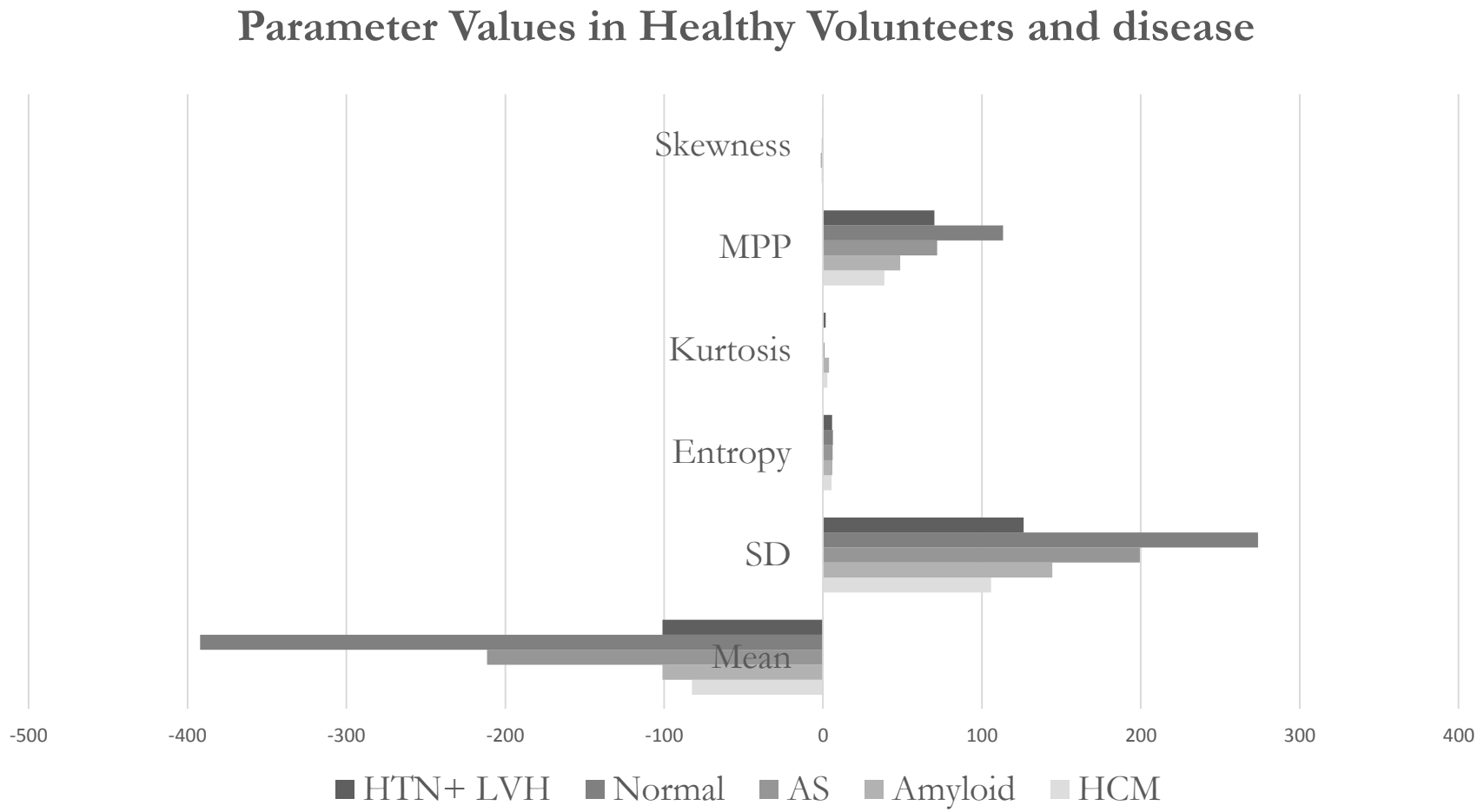

Table 1: A table outlining all the CMRTA derived texture parameters and their meaning.

PARAMETER	DEFINITION
MEAN	The average value of the pixels within the region of interest
SD	A measure of how much variation or dispersion exists from average (mean value). A low SD indicates that the data points tend to be very close to the mean; high SD indicates that the data points are spread out over a large range of values
SKEWNESS	A measure of the asymmetry of the histogram. The skewness value can be positive or negative. A negative skew indicates that the tail on the left of the histogram is longer than the right ride. A positive skew indicates that the tail on the right side is longer than the left side. A zero value indicates the values are both evenly distributed on both sides of the mean
KURTOSIS	A measure of the peakedness of the histogram. The kurtosis can be positive or negative. A positive kurtosis indicates a histogram that is more peaked than Gaussian (normal) distribution. A negative kurtosis indicates that the histogram is flatter then a Gaussian distribution
ENTROPY	A marker of randomness
MEAN POSITIVE PIXEL	Considers only pixels greater than zero and so reduced the impact of dark objects on the mean histogram value.

Table 2: Table showing the absolute values to 2 decimal places of the 6 parameters for each of the disease states and HV, using Spatial Filter Size 3.

SPATIAL FILTER SIZE	PARAMETERS	HCM	AMYLOID	AS	NORMAL
SSF3	Mean	-82.48	-101.07	-211.43	-392.07
	SD	105.79	144.35	199.47	273.76
	Entropy	5.39	5.81	6.02	6.22
	Kurtosis	2.64	3.81	1.05	-0.03
	MPP	38.65	48.61	71.78	113.32
	Skewness	-0.94	-1.43	-0.74	-0.00

Table3: Table showing the pair-wise comparison of all study cohorts and the parameters showing statistical significance

Pair Wise Comparison	***Parameters showing significant differences***	***Parameters not meeting statistical significance***
HCM vs CA	SD, entropy	Mean, skewness, MPP, kurtosis
HCM vs AS	Mean, SD, MPP, entropy, kurtosis	Skewness
CA vs AS	Mean, SD, MPP, entropy, skewness, kurtosis	
HCM vs HTN+LVH	Skewness, MPP	Mean, SD, entropy, kurtosis
CA vs HTN+LVH	Skewness	Mean, SD, MPP, entropy, kurtosis
AS vs HTN+LVH	Mean, SD, entropy,	Skewness, MPP, kurtosis

- Textural Analysis provides additional information from routinely acquired medical imaging.

- Textural Analysis can be performed on a single frame bSSFP cine image which are routinely acquired in routine CMR.

- CMRTA ‘knows’ the difference between health and disease and shows promise in differentiating between diseases causing LVH.

- Large volume analysis of CMR datasets using TA, combined with machine learning, shows promise as an ancillary diagnostic tool and possibly a prognostic indicator.